CHARACTERIZATION OF LUNAR POLAR AND NON-POLAR PERMANENT SHADOW PHYSICAL AND THERMAL CHARACTERISTICS VIA MINI-RF AND DIVINER. J.T.S. Cahill[1], M.A. Siegler[2], B.T. Greenhagen[2], D.B.J. Bussey[1], J.A. McGovern[1], and M. Even[1], [1]The Johns Hopkins University Applied Physics Laboratory, Laurel MD 20723, [2]Jet Propulsion Laboratory, California Institute of Technology, Pasadena CA.

Introduction: In recent geologic history, as a result of the angular separation of the lunar polar axis remaining less than ~1.59° relative to the normal of the ecliptic plane [2] sub-solar latitudes have remained low maintaining a perpetual shadow in many crater interiors at the poles for millions, possibly billions of years. These characteristics persuaded *Watson* [3] to postulate that any volatiles on the lunar surface might well get cold-trapped within these permanently shadowed regions (PSR). Many have examined this possibility with a varying array of instrumentation and methods and achieved varying degrees of success attempting to prove water could be present in these regions (e.g., [4-9]). However, it was not until recent additional corroborative observations by M^3, VIMS, HRI-IR, LAMP, LCROSS, as well as S-band radar measurements by the Mini-SAR were presented that more comprehensive evidence confirmed the presence of OH^-/H_2O at the Moon's poles [10-15].

Siegler et al. [16] and *Schorghofer and Taylor* [17] have suggested that many PSRs may be too cold to enable volatiles enough mobility to move downward into the regolith for cold-trap capture; leaving only a space weathering driven surficial volatile mobility regime [18-20]. If non-thermal loss processes (e.g. cosmic rays, Lyman-alpha light) are more efficient than burial processes, ice will not concentrate in the subsurface. It remains unclear if non-thermal burial will be fast enough to bury ice at the rate it is supplied to the lunar cold traps.

However, recently discovered PSRs outside the immediate vicinity of the lunar polar regions (as low as ±58°) may be more optimal for temperature driven volatile mobility, trapping, and storage [1] (**Fig. 1**). These areas, labeled "lunar permafrost" by *Paige et al.* [21], or optimistically "ice traps" by *Siegler et al.* [16] would exceed the 100 K maximum temperature generally used to define cold traps [17, 22, 23]. Previous thermal stability modeling suggests that these regions may be efficient ice collectors even when mean temperatures exceed 150 K. Here we begin an examination of polar and non-polar PSRs to characterize their physical and thermal properties at varying latitudinal conditions for a greater understanding of volatile stability in lunar PSRs.

Methodology: *Lighting*— We leverage the lighting maps constructed by *McGovern et al.* [1] which precisely simulate lunar illumination conditions to locate PSRs in each hemisphere from pole to ±58° using a merged LOLA and LROC WAC stereo DTM [1, 24, 25]. With their locations well established, here we begin to characterize them for temperature and radar surface scattering properties at varying distances from the poles. A more explicit explanation of how these maps are constructed and

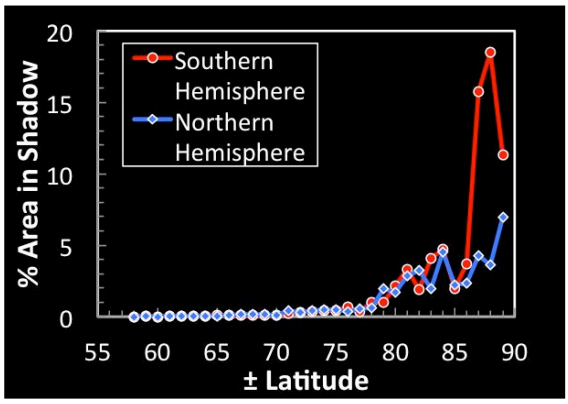

Figure 1: *Total percentage area in permanent shadow by latitude* [1].

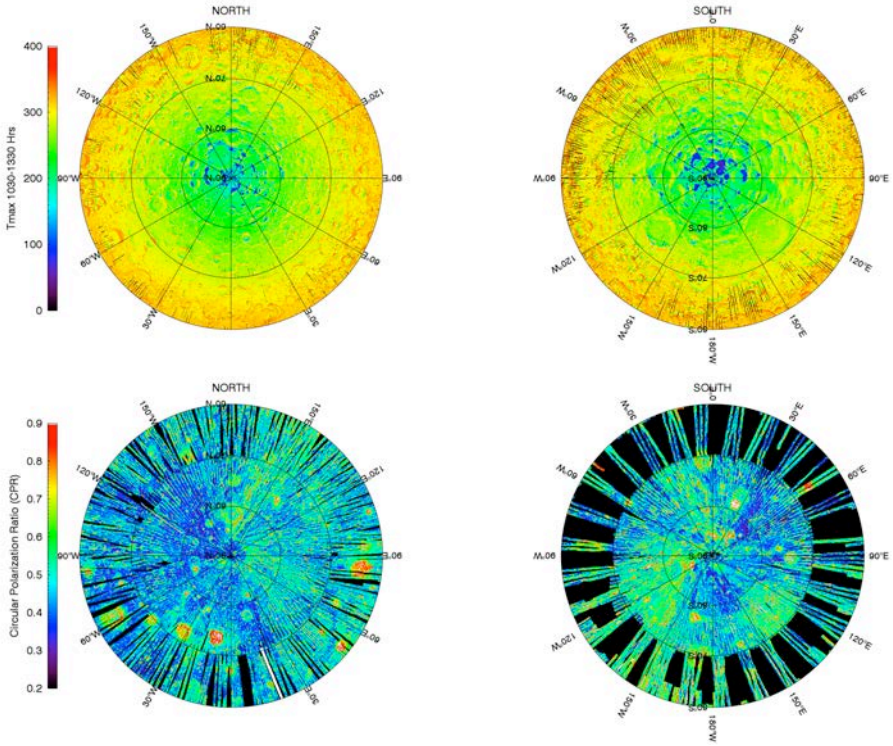

Figure 2. *Polar stereographic (16 ppd) views of the southern (left) and northern (right) hemispheres (± 60° to 90°) showing (top) DIVINER $T_{max1030-1330}$ and (bottom) Mini-RF CPR.*

where polar and non-polar PSRs are located is detailed in *McGovern et al.* [1].

DIVINER—Average and maximum temperature information is determined using data collected by the LRO DIVINER Lunar Radiometer instrument [26] (**Fig. 2**). DIVINER measures reflected solar and emitted infrared radiation in nine channels from 0.3 to 400 μm [26]. Previous polar temperature studies of permanent shadows suggest temperatures ranging between ~40 to 90 K [21]. However, initial temperature data for the non-polar PSRs (e.g., near Pythagoras central peak) suggests temperature conditions (<160 K), still consistent with PSRs and roughly consistent with temperature driven volatile cold trapping.

Mini-RF S-Band—Mini-RF is a hybrid-polarized, side-looking, synthetic aperture radar (SAR) that has collected ~99% coverage of each pole in S-band (12.6 cm) and X-band (4.2 cm) wavelengths [27, 28] (**Fig. 2**). Here, we concentrate our analysis on S-band zoom data products that are sensitive to materials 0.1 to 1.26 meters in size and similar vertical depths. Mini-RF collects four Stokes parameters (S_1, S_2, S_3, S_4), or quantitative measurements of polarized radar energy scattered from the lunar surface [29, 30]. Mini-RF data can then be used to compute several analytically valuable child parameters that, in this context, are useful for discerning the presence of relatively coherent deposits of ice. This is typically done via examination of circular polarization ratio (CPR), where typically high CPR values will be used as a discriminator for surface roughness and ice. The circular polarization ratio is defined as the ratio of the same sense (SC) relative to the opposite sense (OC) polarized returns.

Results: A preliminary macroscopic characterization of all PSR regions for surface temperature and radar scattering characteristics show northern hemisphere PSRs to have mean T_{avg} of 79.8 K and mean T_{max} of 159.4 K (**Fig. 3**). Radar bright regions in northern hemisphere PSRs are characterized with mean temperatures that are actually warmer with mean T_{avg} and T_{max} values showing 91.6 and 186.5 K, respectively. Southern-hemisphere radar bright regions within PSRs are also characterized with warmer temperatures (mean T_{avg} = 85.6 K and T_{max}= 145.9 K) relative to southern-hemisphere temperatures as a whole (mean T_{avg} = 72.5 K and T_{max}= 125.3 K).

Summary and Future Work: The results reported herein are very preliminary, but show a relatively modest areal proportion of lunar PSRs to be radar bright. Of these radar bright PSRs, average and maximum temperatures are generally warmer than PSRs as a whole. However, southern-hemisphere radar bright regions are characterized with temperatures that are well within proper conditions for volatile sequestration. In contrast, northern hemisphere radar-bright PSRs have average maximum temperatures that may be too high for sustained volatile sequestration. This does not negate the plausibility of ice in northern hemisphere polar PSRs which do have suitable temperatures for volatile sequestration. Future work will examine T_{avg}, T_{max}, and CPR characteristics with varying latitude.

References: [1] McGovern J.A. et al. (2012) Icarus, accepted. [2] Spudis P.D., *The once and future Moon*. 1996, 308. [3] Watson K. et al. (1961) JGR, 66, 1598-1600. [4] Arnold J.R. (1979) JGR, 84, 5659-5668. [5] Feldman W.C. et al. (1998) Science, 281, 1496-1500. [6] Feldman W.C. et al. (2000) JGR, 105, 4175-4195. [7] Feldman W.C., et al. (2001) JGR-Planets, 106, 23231-23251. [8] Bussey D.B.J. et al. (2010) Icarus, 208, 558-564. [9] Mazarico E. et al. (2010) Icarus, doi: 10.1016/j.icarus.2010.10.030. [10] Pieters C.M., et al. (2009) Science, 326, 568-572. [11] Clark R.N. (2009) Science, 326, 562-564. [12] Sunshine J.M. et al. (2009) Science, 326, 565-568. [13] Gladstone R.G. et al. (2012) JGR-Planets, 117, doi:10.1029/2011JE003913. [14] Spudis P.D. et al. (2010) GRL, 37. [15] Colaprete A. et al. (2010) Science, 330, 463-468. [16] Siegler M.A. et al. (2011) JGR-Planets, 116, doi: 10.1029/2010JE003652. [17] Schorghofer N. and Taylor G.J. (2007) JGR, 112. [18] Crider D.H. and Vondrak R.R. (2003) Moon: Science, Exploration and Utilisation, 31, 2293-2298. [19] Crider D.H. and Vondrak R.R. (2003) JGR-Planets, 108, -. [20] Hurley D.M. et al. (2012) GRL, submitted. [21] Paige D.A. et al. (2010) Science, 330, 479-482. [22] Watson K. et al. (1961) JGR, 66, 3033-3045. [23] Vasavada A.R. et al. (1999) Icarus, 141, 179-193. [24] Riner M.A. et al. in *AGU Fall Mtg.* 2011. San Francisco, CA. [25] Scholten F. in *EPSC-DPS Joint Meeting*. 2011. Nantes, France. [26] Paige D.A. et al. (2010) SSR, 150, 125-160. [27] Chin G. et al. (2007) Space Science Reviews, 129, 391-419. [28] Nozette S. et al. (2010) SSR, 150, 285-302. [29] Campbell B.A. et al. (2007) IEEE Trans. Geo. Rem. Sen., 45, 4032-4042. [30] Raney K. (2006) Geosci. Rem. Sens. Lett., 3, 317.

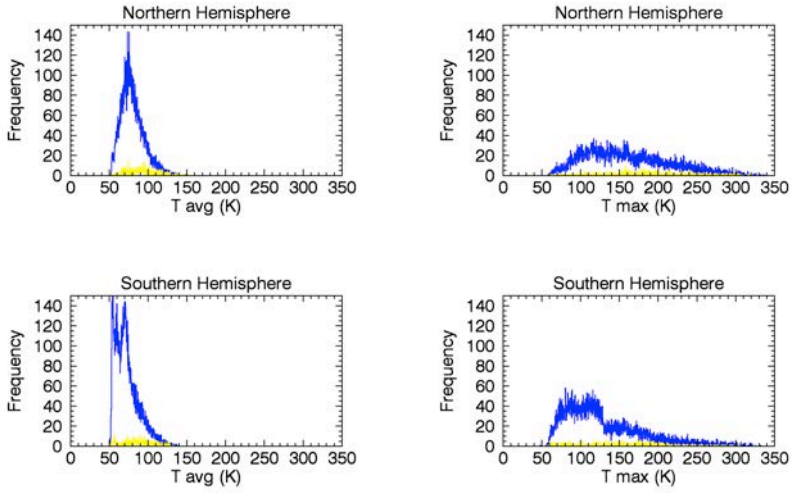

Figure 3: *In blue is DIVINER mean and maximum temperature statistics for PSRs in the northern (top) and southern (bottom) hemispheres. In yellow is DIVINER mean and maximum temperature statistics for PSRs that host radar bright materials as seen by Mini-RF.*